

CHAPTER VII

RESIDUE CATALYST SUPPORT REMOVAL AND PURIFICATION OF CARBON NANOTUBES BY NaOH LEACHING AND FROTH FLOTATION*

7.1 Abstract

The synthesis of carbon nanotubes (SWNTs) by the catalytic decomposition of gaseous carbon-containing molecules has been considered to be the most promising process for large-scale production with a relatively low cost. However, the as-prepared SWNTs from this process always contain significant amounts of impurities such as metallic catalysts, catalyst support, and other unwanted forms of carbon. For a variety of potential applications, the purification of SWNTs is considered to be an important step. In this research, NaOH solution was utilized to dissolve the silica support, a major impurity, from the SWNTs produced by the CO disproportionation over a CoMo/SiO₂ catalyst. Subsequently, froth flotation was used to further recover and concentrate the total carbon after the NaOH pretreatment. To achieve a high purity of total carbon by the proposed purification techniques, the effects of operating parameters such as sonication time, initial surfactant concentration, solid loading, air flow rate, and initial foam height were investigated in order to minimize the entrainment of undissolved silica with the froth. The purity of total carbon was found to increase to 30% after the first step of NaOH treatment and to 78% after the second step of froth flotation as compared to the initial carbon content of only 4% of the as-prepared SWNTs. From the TPO results, the Raman spectra and the SEM images, the physical and chemical structures of SWNTs are not damaged by NaOH treatment and froth flotation.

7.2 Introduction

In 1993, Sumio Iijima discovered single-walled carbon nanotubes (SWNTs) which were produced by using the arc-discharge technique [1]. Since then, SWNTs have become of great interest and have been investigated extensively because they

* Published in the Journal of Separation and Purification Technology

have outstanding electrical, mechanical, and thermal properties [2, 3]. Currently, there are three processes to produce SWNTs – arc-discharge [1, 4], laser vaporization [5], and heterogeneous catalytic reaction [6]. The first two processes are limited for scaling up to commercial production due to the requirement of high temperatures and the complicated development for a continuous system, while the heterogeneous catalytic process not only requires moderate temperatures but it is also easy to set up. Therefore, the production of SWNTs by using the heterogeneous catalytic reaction has been considered to be a promising approach for a large scale production. However, the yield of produced SWNTs from this process is not yet satisfied since the as-produced SWNTs still contain a large fraction of the catalyst support [7]. To scale up the heterogeneous catalytic reaction process for a commercial production, the purification of the SWNTs produced by this technique has to be considered as a crucial step. In this research, the SWNTs produced from the CO disproportionation over a Co-Mo catalyst using a silica support were used in the purification experiment. One interesting method to purify SWNTs is to oxidize the spent catalysts and then to follow by acid treatment such as with HCl [8, 9] or HNO₃ [10, 11] for metallic catalysts removal. HF or NaOH was also used for removing silica support [12]. Even though HF is the most effective chemical to dissolve silica, it is extremely dangerous and very difficult to handle because it can burn the eyes, skin, and mucous membranes [13]. Therefore, it is not practical to use HF in a large scale SWNT purification. The use of a membrane is also considered to be a potentially viable technique to concentrate SWNTs. However, the membrane filtration technique also has some drawbacks, such as high material cost, and fouling build up.

Froth flotation is a separation technique that uses a surfactant as a means of separation; called a surfactant-based separation process [14]. It has been widely used in the area of mineral processing [15]. In a froth flotation operation, air is introduced at the bottom of a flotation column to generate foam, which is the critical issue in this technique [16] since SWNTs can co-adsorb preferentially at the bubble surface rising to the top of the column. A surfactant added to the solution plays an important role to generate foam as well as to stabilize the produced foam on which both solid particles and surfactant concentrate. The reasons for selecting the froth flotation technique to

selectively separate and concentrate SWNTs are its outstanding features of rapid operation, low space requirement, high removal efficiency, and low cost of operation [17].

In our previous work [18], froth flotation was applied to separate carbon black, a model of SWNTs, from silica gel. In that study, the separation of carbon black from silica gel was done by using a nonionic surfactant (ethoxylated alcohol) because the PZCs of these two solid particles are not significantly different (the PZC of carbon black is 3.5 and the PZC of silica gel is 4.1). It was reported that a higher than 70% separation efficiency of carbon black was achieved by using froth flotation. However, carbon black was easily separated from silica gel by froth flotation because carbon black and silica gel were physically blended together. In contrast to the mixture of carbon black and silica gel, there are strong interactions between the SWNTs and the silica support in the as-prepared SWNT sample since the SWNTs were synthesized by growing on the silica surface [19]. Therefore, in the present study, NaOH was used for silica dissolution prior to the step of SWNT recovery by froth flotation. An ethoxylated alcohol nonionic surfactant was selected again for running the froth flotation experiments.

7.3 Experimental Section

7.3.1 Materials

7.3.1.1 *Metal Precursors and Catalyst Support*

Cobalt(II) nitrate hexahydrate ($\text{Co}(\text{NO}_3)_2 \cdot 6\text{H}_2\text{O}$) with a purity above 98% and ammonium molybdate tetrahydrate ($(\text{NH}_4)_6\text{Mo}_7\text{O}_{24} \cdot 4\text{H}_2\text{O}$) with 81.0-83.0% as MoO_3 were used as catalyst precursors. Silica gel (SiO_2) was used as a catalyst support and having particle sizes in the range of 70-230 mesh (62-210 μm) with an average pore diameter of 6 nm, a BET surface area of 480 m^2/g , and a pore volume of 0.75 cm^3/g . All the catalyst precursors and the catalyst support were supplied by Sigma-Aldrich Co. Ltd. NaOH with a purity above 97%, obtained from Carlo Erba Company, was utilized to dissolve the silica support from the as-prepared SWNTs. Linear ethoxylated alcohol with seven mole ethoxylate of linear, primary

12-14 carbon number alcohol, Surfonic@ L24-7, a nonionic surfactant, obtained from Huntsman Company, was used as a froth agent in the froth flotation operation. All chemicals were used as received without any further purification. Deionized water was used in preparing all aqueous solutions.

7.3.1.2 Gases

Air zero was used in the catalyst calcination. Hydrogen, with a purity of 99.99%, was used for the pre-reduction of the catalyst in the SWNT synthesis step. Helium, with a purity of 99.99%, was used as an inert gas in the heating step of the SWNT synthesis. 2% oxygen in helium balance was used as an oxidizing agent in the temperature-programmed oxidation (TPO) experiment. All of the above gases were supplied by Thai Industrial Gas Co. Ltd. Carbon monoxide gas, with a purity of 95%, was obtained from Airgas Inc. It was used as a carbon source for the SWNT synthesis.

7.3.2 Methodology

7.3.2.1 Synthesis of SWNTs

The SWNTs used in this study were synthesized by using the disproportionation of carbon monoxide gas over a bimetallic catalyst of cobalt and molybdenum oxides supported on silica gel (Co-Mo/SiO₂). The Co-Mo/SiO₂ catalyst used was prepared at an optimum molar ratio of Co to Mo of 1:3 and had a total metal loading of 6 wt.% [7]. An amount of the calcined catalyst (0.3 g) was placed in an 8-mm horizontal tubular reactor, heated in a H₂ flow to 500°C, held on this temperature for 30 min, and then heated in a He flow to 850°C. Subsequently, CO was introduced at a flow rate of 850 cm³/min at 5 atm and the reactor was kept under these conditions for 30 min. At the end of the reaction, the spent catalyst sample was taken for determining carbon yield, classifying the type of deposited carbons, and observing the morphology of the deposited carbons, including SWNTs, by using TPO, Raman spectroscopy, and scanning electron microscope (SEM). The procedures of carbon yield measurement by TPO are available elsewhere [20]. The

Raman spectra were obtained in a Raman spectroscopy (Jovin Yvon-Horiba Lab Ram) equipped with a charge-coupled detector and with He-Ne laser (632 nm) as excitation source. The SEM, JOEL model JSM-5200-2AE, was used to examine the morphological change after the silica dissolution and froth flotation steps, at the magnification of 10,000 times and an acceleration voltage of 15 kV.

7.3.2.2 Silica Dissolution Experiments

A different quantity of the as-prepared SWNT sample in the range of 0.2-1.4 g was mixed with 30 ml of a 10 M NaOH solution in a vial. This mixture was sonicated in a 440W ultrasonic bath (Crest, 575DAE) at different sonication times. To minimize the loss of carbons from the sample, the mixture was added, after the sonication was completed, to a nonionic surfactant solution without removing the remaining NaOH in the silica dissolution step for further SWNT sample purification and concentration by froth flotation. In order to determine the total amount of carbons in the NaOH-treated SWNT sample, the basic sonicated mixture was neutralized by HCl solution to obtain a pH value of 7 ± 1 and was centrifuged at 15,000 rpm for 20 min. The solid was then dried at 110°C to determine the total dried weight. The TPO, Raman spectroscopy, and SEM experiment were used to measure the carbon content and to observe the morphological change of carbons in the sample.

7.3.2.3 Froth Flotation Experiments

A schematic of the froth flotation apparatus used in this work is shown in Figure 7.1. The flotation column was a glass column with an internal diameter of 4.1 cm and a height of 75 cm. Filtered air was introduced at the bottom of the column through a sintered glass disk having pore size diameters of 40-60 μm . In order to determine the effects of foam height, surfactant concentration, and solid loading, a quantity of 300-700 ml of solutions containing different concentrations of the NaOH-pretreated SWNTs and surfactant was poured into the froth flotation column. To investigate the effect of air flow rate on the SWNT separation efficiency, the air flow rate was varied from 40 to 120 ml/min by using a mass flow controller.

The froth flotation experiments were operated in batch mode at room temperature ($25\pm 1^\circ\text{C}$) and the operation was terminated when, due to surfactant depletion, no foam came out from the top of the column. The generated foam was collected at the top of the column and was then allowed to collapse. The collapsed foam was then washed to remove the surfactant by rinsing with deionized water and centrifuging at 15,000 rpm for 20 min. This surfactant-washing step was carefully repeated several times until there was no visible foam in the sample solution. The sample solution was then dried overnight in an oven at 110°C to determine the total dried weight. The TPO, Raman spectroscopy, and SEM experiment were used to measure the carbon content and to observe the morphological change of carbons in the sample.

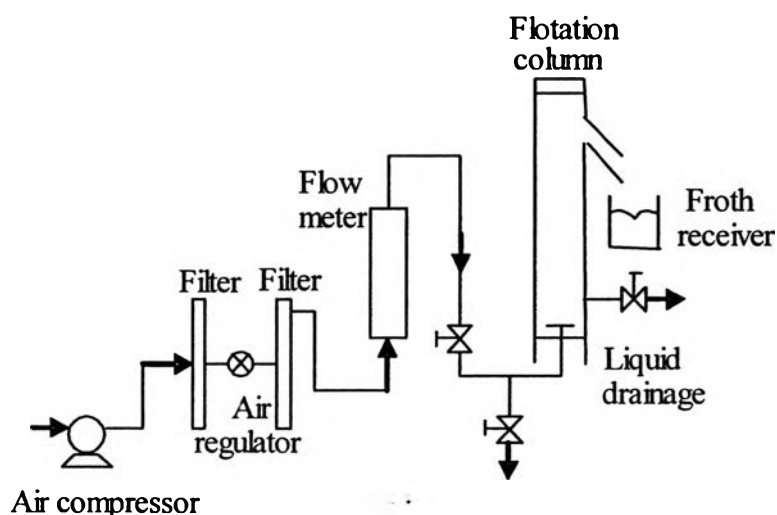


Figure 7.1 Schematic of the froth flotation apparatus.

7.3.2.4 Foam Characteristic Experiments

Foam characteristic experiments were also conducted independently in an extended flotation column having the same internal diameter and porosity of the sintered glass disk. After a solution having different concentrations of the NaOH-treated SWNT sample and the surfactant was transferred to the column and well mixed, filtered air was introduced at the bottom of the column at a desired flow rate. The maximum foam height divided by the initial solution height in the column is defined as foamability. After the maximum foam height was attained, the flow of air to the column was then stopped and the time required for the foam

volume to collapse to one half of the maximum height was used to quantify foam stability ($t_{1/2}$).

7.4 Results and Discussion

In this work, the carbon content of the sample is defined as the weight of the combustible fraction as a percentage of the total solid, where the combustible fraction in the total solid was calculated from the peak area under the TPO curve [20]. From the TPO results, the carbon content of the as-prepared SWNT sample was measured to be around 4%, in which it contained a disordered carbon fraction of 0.25 and an SWNT fraction of 0.75 (see details in section 7.4.6). The carbon content of the sample, after silica removal by using 30 ml of 10 M NaOH solution with a sonication time of 3 hours, increased to around 30%. The NaOH-treated SWNT sample was further purified and concentrated by using froth flotation. The initial pH value of the feed solution was found to be high, in the range of 13.0-13.5, due to the remaining NaOH in the silica removal step. Since the froth flotation was performed under high solution pH values, the surfaces of both the SWNTs and the silica gel become negatively charged because the point of zero charges (PZCs) are 7.0 for SWNTs [8] and 4.1 for silica gel [18], which are much lower than the solution pH values. Hence, a nonionic surfactant was used as a frother instead of an ionic surfactant. The CMC of the studied surfactant is 82.1 μM [18], which is in good agreement with literature CMC values for this type of surfactant structure [21]. In the froth flotation operation, the surfactant present in the system can adsorb on all surfaces, including SWNTs, silica, and air bubbles. The amount of surfactant at the air/water interface is generally negligible, when compared to the total amount of surfactant [18]. Since a high purity of SWNTs cannot be obtained, the adsorption isotherms of the studied surfactant on the surface of SWNTs are not available in this study. The fraction of recovered carbons in the overhead froth divided by the fraction of carbons that is originally in the initial feed to the froth flotation column is defined as the enrichment ratio of total carbon. To achieve an effective froth flotation operation, the enrichment ratio has to be higher than unity. Apart from the carbon content and the enrichment ratio, the recovery of total carbon is also another

important parameter in assessing the efficiency performance in the froth flotation operation. Under the studied conditions, the recovery of total carbon by froth flotation was found to be higher than 80%. However, correlations between the recovery and the studied operating parameters are not reported here. This is because a significant amount of the entrained carbon was found to adhere to the wall of the column during the froth flotation operation, leading to inaccurate calculations of the total carbon recovery. Therefore, the carbon content and enrichment ratio of total carbon are only used to evaluate the effects of operating parameters on the process performance of froth flotation in this study.

7.4.1 Effect of Sonication Time

To achieve the effective separation of SWNTs in the froth flotation operation, pretreatment of the silica dissolution with sonication was performed to break-up the strong interactions between the SWNTs and the silica support, as well as to dissolve certain fraction of silica. As shown in Figure 7.2, the carbon content increases slightly with increasing sonication time and then it tends to reach a plateau at 14 h of sonication time. Increasing sonication time can break the interaction between the SWNTs and the silica support so more silica can be dissolved by NaOH, leading to higher carbon content. However, increasing sonication time above 14 h did not improve either the carbon content or enrichment ratio, even though the added NaOH is several times in excess with the amount of silica in the sample, indicating that the dissolution rate of silica by NaOH approaches zero because some of the silica gel is completely covered by the carbons. Figure 7.2 also shows the enrichment ratio as a function of sonication time. Like the carbon content, the enrichment ratio reached a maximum of approximately 3.0 at 14 h of sonication time. It is interesting to note that the enrichment ratio was found to be much higher than unity in all studied sonication times. Since the carbon content at 3 h sonication time was slightly lower than that at 14 h of sonication time, a sonication time of 3 h was selected for further experiments to investigate other operating parameters of froth flotation.

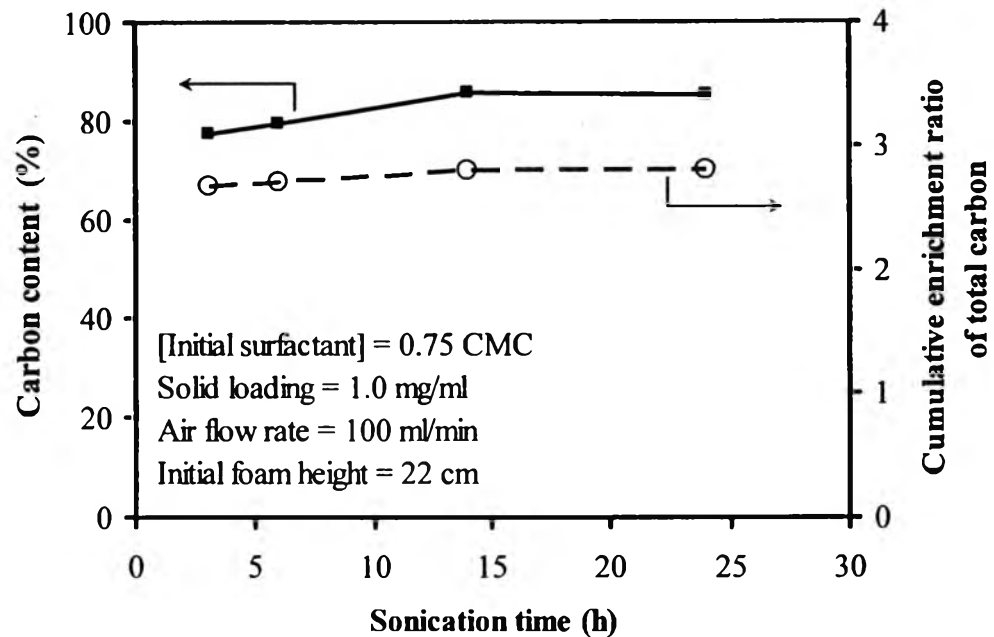


Figure 7.2 Effects of sonication time in the silica dissolution step on carbon content and cumulative enrichment ratio of the SWNT sample in the froth flotation step.

7.4.2 Effect of Initial Surfactant Concentration

In a froth flotation operation, a surfactant plays an important role in both promoting and stabilizing the foam [22]. In addition, the separation efficiency was found to be highest at a surfactant concentration which corresponds to the maximum values of both foamability (foam formation) and foam stability [23-24]. Figure 7.3a shows the effect of initial surfactant concentration on foam characteristics. As the surfactant concentration increased, foamability significantly increased; whereas foam stability monotonically decreased. It can be seen that the maximum foamability appeared at around the CMC, which is generally observed in other surfactant systems [25]. However, the relationship of foam stability to surfactant concentration is more complicated and system-dependent.

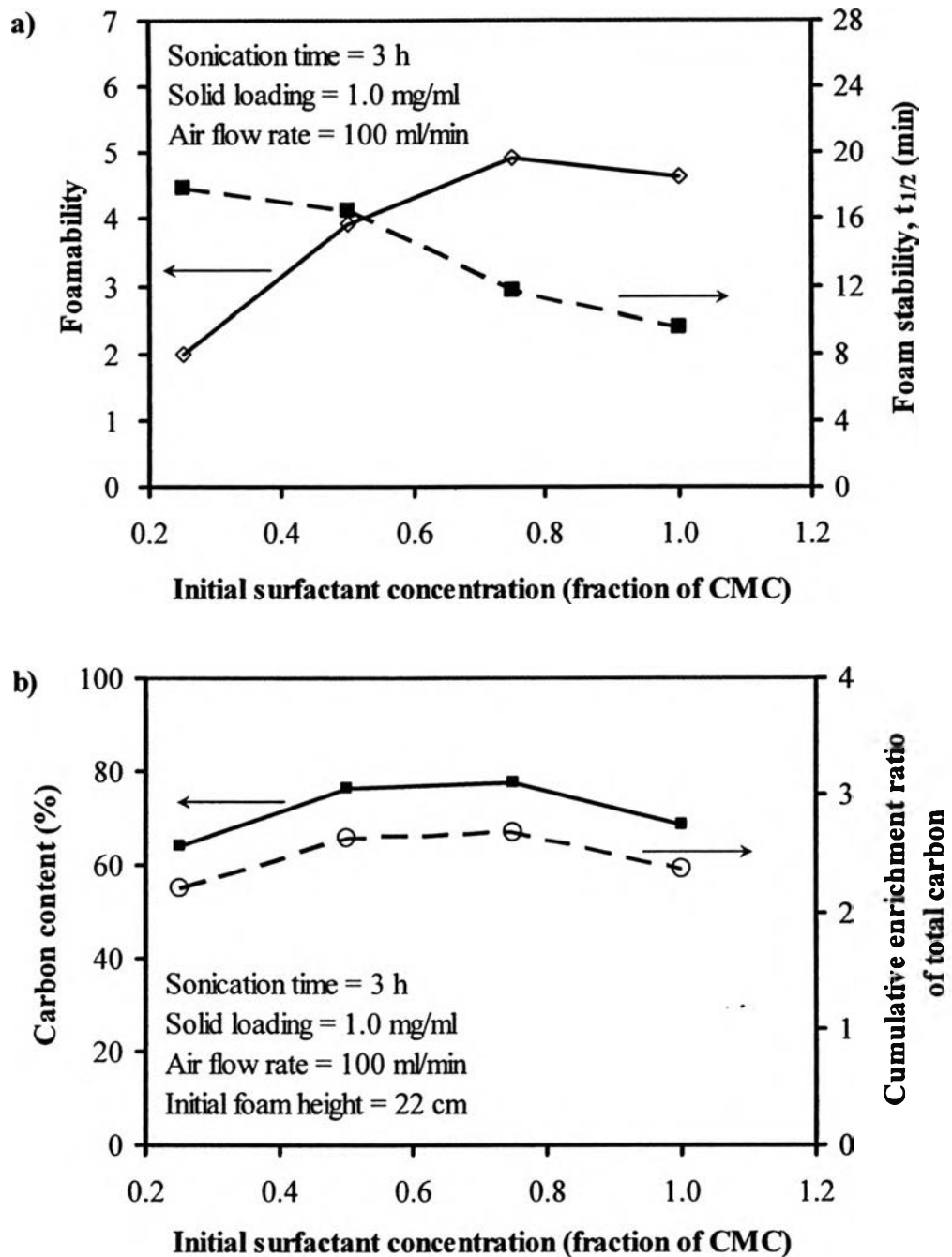


Figure 7.3 Effects of initial surfactant concentration on (a) foamability and foam stability, and (b) carbon content and cumulative enrichment ratio of the SWNT sample in the froth flotation step.

As shown in Figure 7.3b, both the carbon content and cumulative enrichment ratio increase with increasing surfactant concentration in the range of 0.25 to 0.75 times the CMC; but when the surfactant concentration approaches the

CMC, both the carbon content and cumulative enrichment ratio tend to decrease slightly. Since the interaction between particles and air bubbles and foam lamellae is complex, a fundamental interpretation of selectivity is difficult. However, by comparing Figures 7.3a and 7.3b, both high foamability and high foam stability are basically needed to achieve a high carbon content and a high cumulative enrichment ratio. The offsetting trends of increasing foamability and decreasing foam stability with increasing surfactant concentration result in an optimum surfactant concentration of around 0.75 times the CMC, so this initial surfactant concentration was used for further investigation in this work.

In the carbon black study [18], increasing surfactant concentration significantly increased the purity of carbon black sample from 40 to 70%. In the case of as-prepared SWNTs, the carbon content as high as 77% (as compared to the initial carbon content of 30%) and the cumulative enrichment ratio of total carbon as high as 3.0 suggest the technical feasibility of froth flotation for the selective separation of the NaOH-treated SWNTs.

7.4.3 Effect of Solid Loading

In order to determine the economically favorable parameters of this froth flotation process, the amount of the NaOH-treated SWNT sample in the feed solution was varied in order to determine an optimum solid loading for a maximum carbon content. The effects of the solid loading of the NaOH-treated SWNT sample (weight of total solids/volume of slurry) in the feed solution on the foam characteristics and the separation efficiency of the froth flotation are shown in Figures 7.4a and 7.4b, respectively. Both foamability and foam stability declined slightly with increasing solid loading. Hydrophobic particles, such as graphite flakes (contact angle with water = 86° [26]) or possibly carbon nanotubes, can act as antifoams or defoamers, while hydrophilic particles, like silica gel (contact angle with water = 4° [27]), can stabilize or destabilize foam [28], so a reduction in foamability and foam stability at high sample loadings is expected.

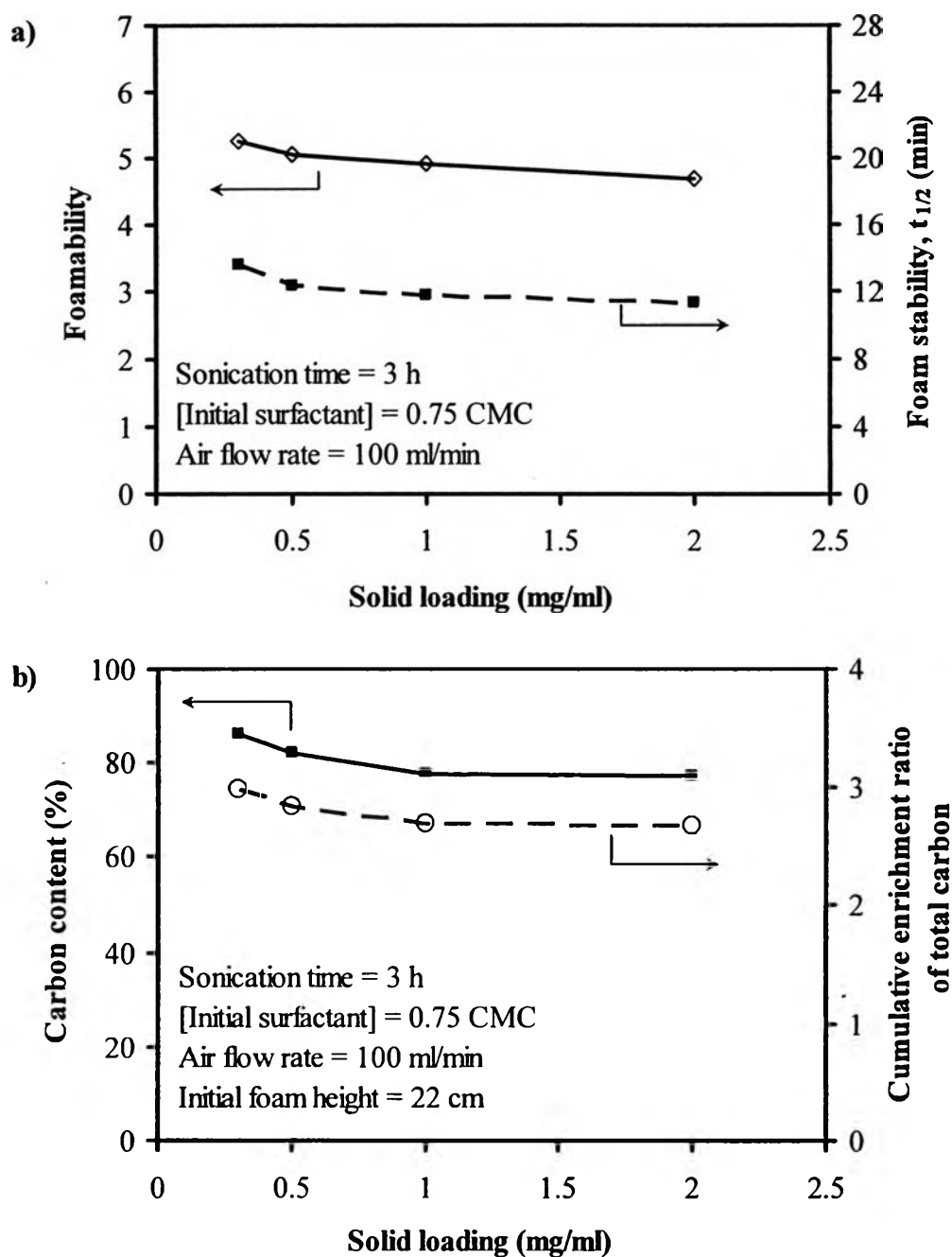


Figure 7.4 Effects of solid loading on (a) foamability and foam stability, and (b) carbon content and cumulative enrichment ratio of the SWNT sample in the froth flotation step.

As shown in Figure 7.4b, the carbon content and cumulative enrichment ratio of total carbon are inversely proportional to the concentration of the NaOH-treated SWNTs in the range of 0.25 – 1.0 mg/ml. However, when the solid

loading increased above 1.0 mg/ml, the carbon content and cumulative enrichment ratio remained almost constant. This is due to the increasing amount of silica in the liquid solution with increasing SWNT concentration.. Since the amount of 10 M NaOH was fixed, the amount of undissolved silica simply increased with increasing SWNT concentration. Consequently, the higher the SWNT sample concentration, the higher the silica fraction in the foam, causing the decrease in separation efficiency. Moreover, the decrease in the carbon content with increasing solid loading is clearly related to the decreases in both foamability and foam stability because the surfactant can adsorb on the surfaces of both the SWNTs and the silica, causing a lower quantity of surfactant monomers available to generate the foam. Based on the results, a solid loading of 1.0 mg/ml was selected for further investigation.

7.4.4 Effect of Air Flow Rate

Air bubbles generated within a liquid solution are used as a means of separation in a froth flotation operation in which SWNT particles attach preferentially on the generated foam [16]. The separation performance of froth flotation relies on volumetric flow rate. The effects of air flow rate on foam characteristics and on the separation efficiency of SWNTs are shown in Figures 7.5a and 7.5b, respectively. To achieve separation, a certain minimum air flow rate is required to cause any of the foam to flow from the top of the column. When the air flow rate increases above the required minimum flowrate, 40 ml/min, foamability gradually increases, whereas foam stability is nearly constant in the studied range, as shown in Figure 7.5a. When the air flow rate increased from 40 to 100 ml/min, the carbon content remained unchanged in the range of 75.5 to 77.5%. However, further increasing the air flow rate above 100 ml/min decreased the carbon content. These results can be explained in that at a very high air flow rate, the circulation velocity induced by the bubble swarm rising through the column is responsible for turbulence at the froth/collection zone interface [29]. Hence, the SWNTs adsorbed at the bubble surfaces can be entrained back to the liquid solution at a very high air flow rate. Similar results are observed in previous froth flotation studies for iron [29] and oil [30] removals.

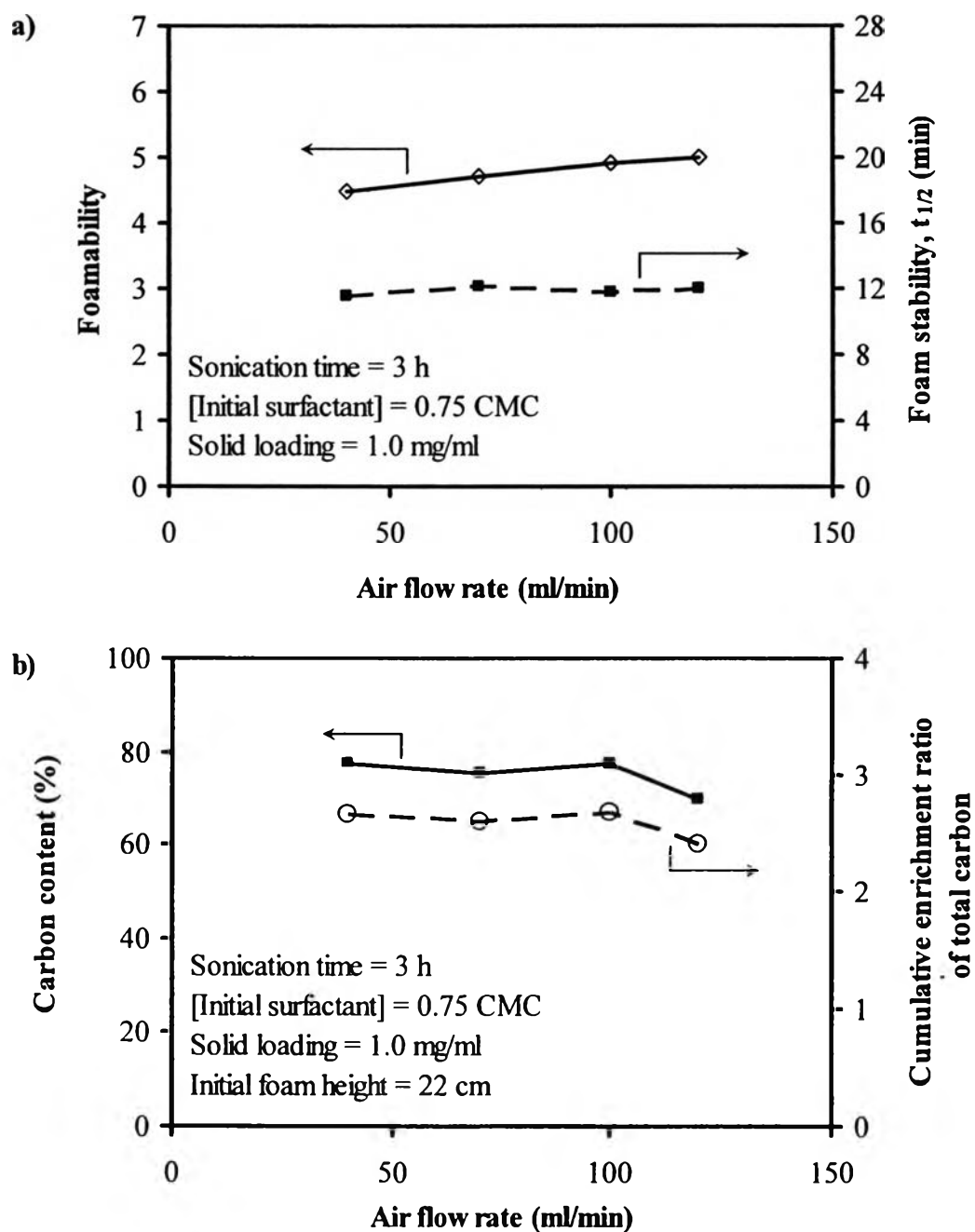


Figure 7.5 Effects of air flow rate on (a) foamability and foam stability, and (b) carbon content and cumulative enrichment ratio of the SWNT sample in the froth flotation step.

For the cumulative enrichment ratio of total carbon, the same trend as the carbon content was observed, and the enrichment ratio above unity was obtained in the studied range of the air flow rate. Since the maximum carbon content and

cumulative enrichment ratio were obtained at an air flow rate of 100 ml/min, it is considered to be the optimum air flow rate for the effective separation and concentration of the NaOH-treated SWNTs.

7.4.5 Effect of Initial Foam Height

There are several methods to improve the selective separation of desired materials, such as adjusting surfactant concentration, salinity, pH, and foam height. The selective separation, in terms of cumulative enrichment ratio, can be improved by increasing the foam height in the column because water within the foam lamellae takes a longer time to drain out of the foam phase [18]. Similar to the carbon black study [18], the carbon content tends to increase with increasing initial foam height in the range of 6 to 50 cm, as illustrated in Figure 7.6.

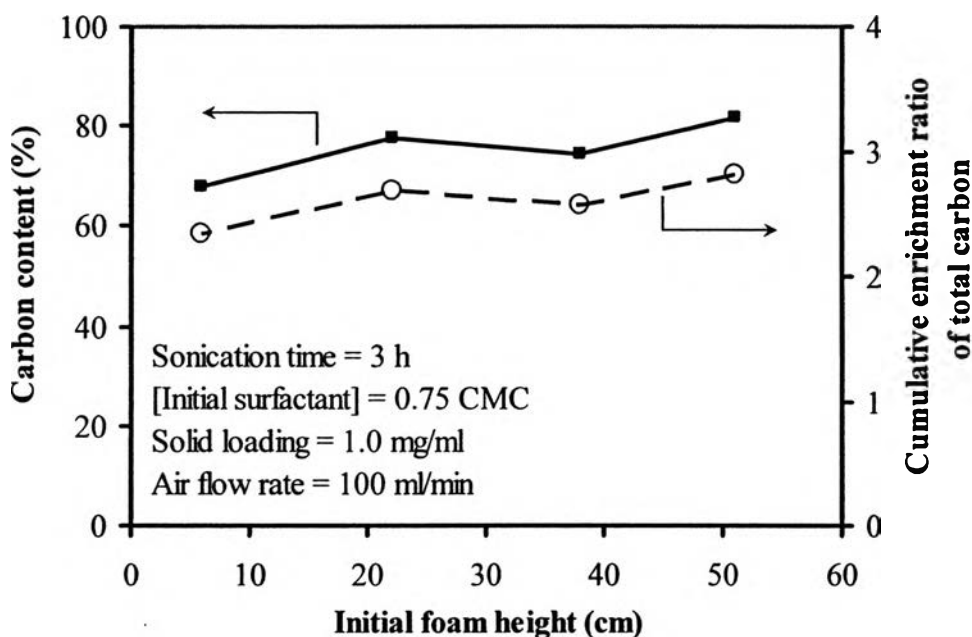


Figure 7.6 Effects of initial foam height on carbon content and cumulative enrichment ratio of the SWNT sample in the froth flotation step.

However, further increasing the foam height above 50 cm was not able to be done in this study because the foam generated never reached the top of the column.

7.4.6 Raman Spectra, TPO Results, and SEM Images of the Sample

The qualification analysis on the structure of carbon in the samples was done by using the information from Raman spectroscopy. The presence of SWNTs in the sample can be directly obtained from the appearance of radial breathing mode (RBM) which occurs below 300 cm^{-1} . Raman signals in the RBM range can also be used to estimate tube diameter of SWNTs [31]. The presence of graphite-like structures, i.e. SWNTs, MWNTs, graphite nanostructure, etc., can be obtained from the appearance of the in-plane stretching mode of ordered crystalline graphite-like structures (G band) that is ranging from $1,400$ to $1,700\text{ cm}^{-1}$. Moreover, the indication on the level of disordered carbon can be obtained from the analysis on the D band which occurs at around $1,350\text{ cm}^{-1}$. The Raman spectra of the as-prepared SWNT sample, the SWNT sample after the silica dissolution step, and the NaOH-treated SWNT sample after the froth flotation step are shown comparatively in Figure 7.7. The full Raman spectra in Figure 7.7a showed that the D band and G band of the three samples are almost identical, where the RBM signals, as shown in Figure 7.7b, have a small different. A small shift of RBM signals, to higher wave number of the two treated samples, is possibly caused by functionalization of the SWNTs by NaOH and/or adsorption of surfactant monomer onto the surface of SWNTs. A strong signal at around 180 cm^{-1} , that can be observed in as-prepared SWNT sample, is almost disappear in the other samples. This signal has been related to the vertically aligned SWNTs that adhere to silica [32]. However, the other signals of higher wave number in RBM range from the treated samples are still remained to indicate that the SWNTs are not destroyed by this purification technique.

The quantification of the different forms of carbon was done by fitting the TPO profiles with gaussian-lorentzian mixtures [20]. The fitted TPO profiles of the as-prepared SWNT sample, the SWNT sample after the silica dissolution step, and the NaOH-treated SWNT sample after the froth flotation step are shown comparatively in Figure 7.8. As can be seen in Figure 7.8, each TPO profile can be split into 3-4 separated peaks by using PeakFit software. The peaks centered around 500 - 530°C represent the carbon in the form of SWNTs [20], where the broad peaks centered at a lower temperature represent the carbon in the form of disordered carbon. It must be noted that the shape and position of a TPO peak may vary when

the catalyst composition changes, and may also vary depending on the kinetics of the oxidation process and the amount of carbon on the surface. Table 7.1 summarizes the carbon compositions of the three different samples calculated from the TPO profiles. From the TPO results, the combined NaOH treatment and froth flotation can provide the enhancement of carbon content, as indicated by the total carbon content increasing from 4% to 30% and to 78% after the silica dissolution step and the silica dissolution/froth flotation step. The percentages of SWNT fractions of the three samples suggest that both NaOH treatment and froth flotation steps do not affect the chemical structure of SWNTs.

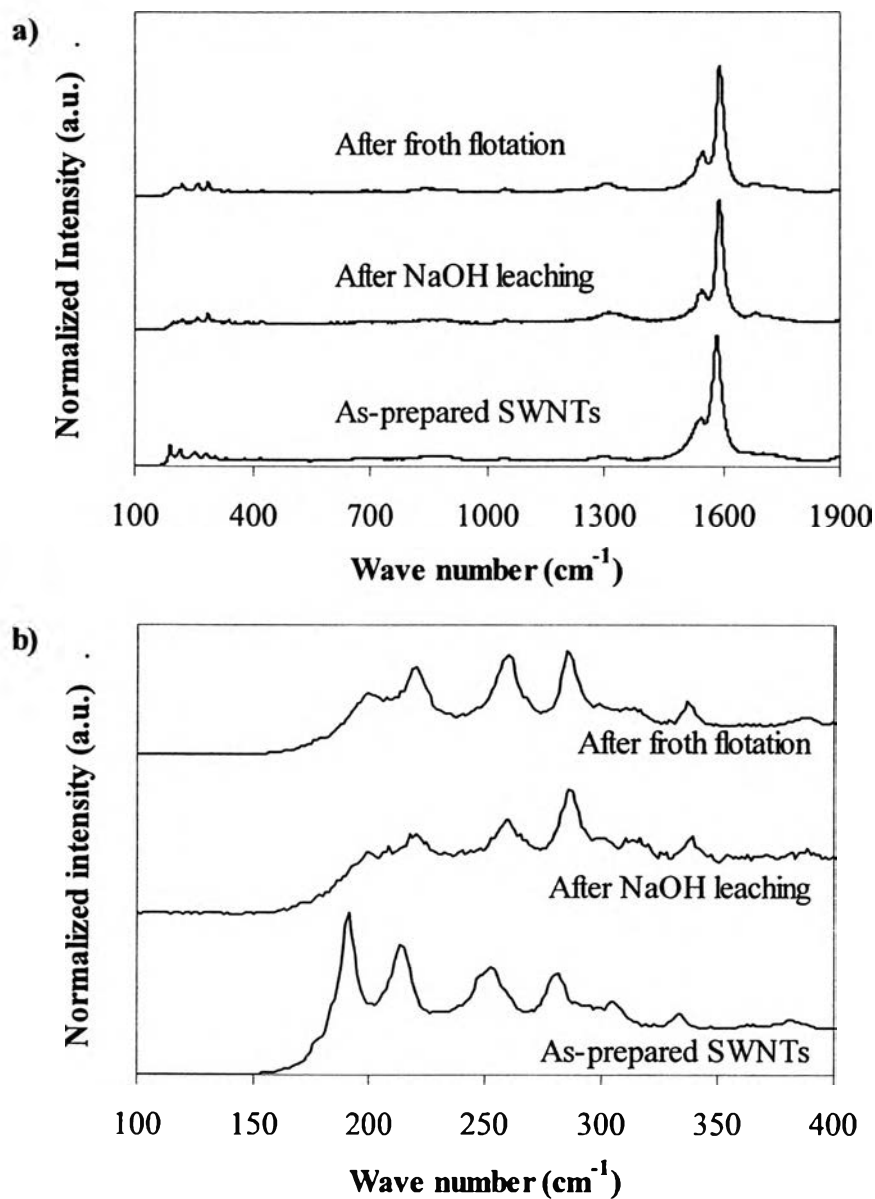


Figure 7.7 Raman spectra of the as-prepared SWNT sample, the SWNT sample after 3 hours of silica dissolution by NaOH, and the SWNT sample after silica dissolution and froth flotation (3 h sonication in the silica dissolution step, 0.75 CMC initial surfactant concentration, 1.0 mg/ml sample loading, 100 ml/min air flow rate, and 22 cm initial foam height).

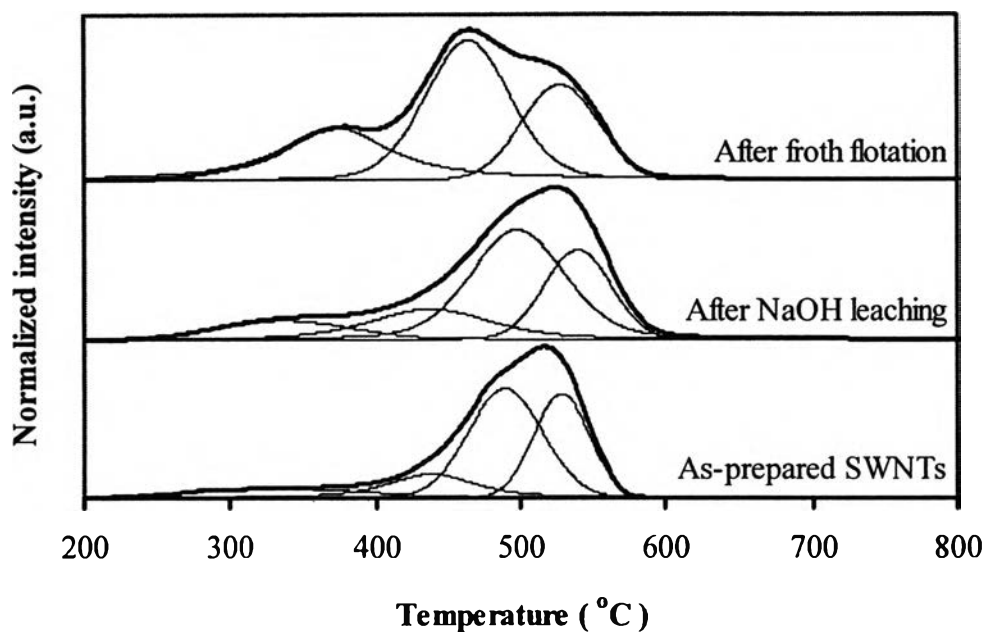


Figure 7.8 Temperature programmed oxidation (TPO) profiles with the peaks fitted by gaussian-lorentzian mixtures for the as-prepared SWNT sample, the SWNT sample after 3 hours of silica dissolution by NaOH, and the SWNT sample after silica dissolution and froth flotation (3 h sonication in the silica dissolution step, 0.75 CMC initial surfactant concentration, 1.0 mg/ml sample loading, 100 ml/min air flow rate, and 22 cm initial foam height).

Table 7.1 Carbon composition and total carbon content as calculated from the TPO data of the as-prepared SWNT sample, the SWNT sample after 3 hours of silica dissolution by NaOH, and the SWNT sample after silica dissolution and froth flotation (3 h sonication in the silica dissolution step, 0.75 CMC initial surfactant concentration, 1.0 mg/ml sample loading, 100 ml/min air flow rate, and 22 cm initial foam height)

Sample	Peak	Peak center	% Area	Type	% Carbon composition	Total carbon content
As-prepared SWNTs sample	1	332	9.6	Disordered carbons	25%	4%
	2	438	14.9			
	3	489	44.5	SWNTs	75%	
	4	528	31.0			
Sample after NaOH dissolution	1	337	10.3	Disordered carbons	28%	30%
	2	437	17.8			
	3	498	47.4	SWNTs	72%	
	4	539	24.6			
Sample after silica dissolution and froth flotation	1	372	28.8	Disordered carbons	29%	78%
	2	464	45.5	SWNTs	71%	
	3	527	25.8			

To observe the changes after the NaOH dissolution and froth flotation steps to purify and concentrate the SWNT sample, SEM images of the as-prepared SWNT sample, NaOH-treated SWNT sample, and the NaOH-treated SWNT sample after the froth flotation step are examined, as shown comparatively in Figure 7.9a-c. Figure 7.9a shows the growth of SWNTs on the surface of silica particles with a

large variety of particle sizes. The diameter of each SWNT bundle was found to be around 0.1 μm (100 nm). From Figure 7.9b, only the large sized silica particles appear dominantly, indicating that most small particles of the silica were dissolved by the NaOH. In comparing the three images, the SWNT fraction increased the most after the froth flotation step. The SEM images also confirm that both the NaOH dissolution and the froth flotation steps do not damage the physical structure of the SWNTs.

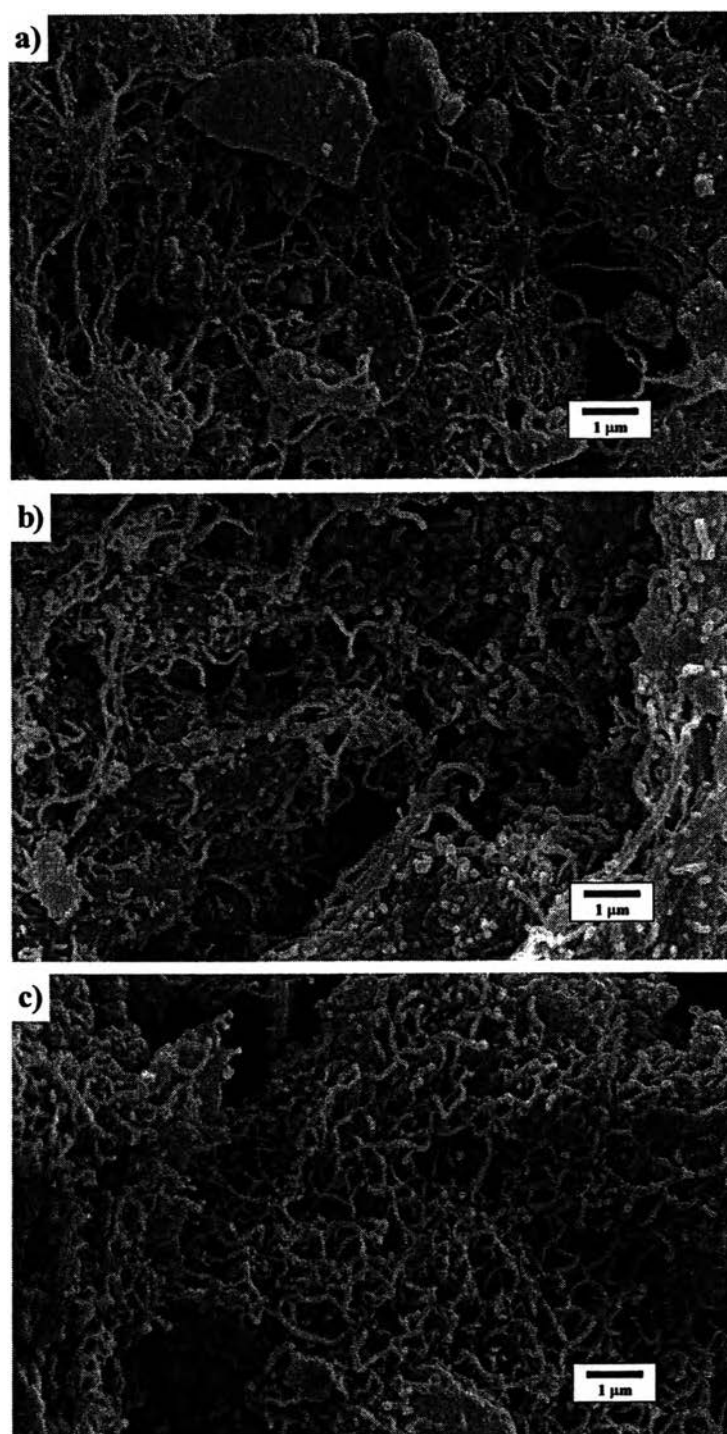


Figure 7.9 SEM images of (a) as-prepared SWNTs, (b) SWNT sample after 3 hours of silica dissolution by NaOH, and (c) SWNT sample after silica dissolution and froth flotation (3 h sonication in the silica dissolution step, 0.75 CMC initial surfactant concentration, 1.0 mg/ml sample loading, 100 ml/min air flow rate, and 22 cm initial foam height).

7.5 Conclusions

Single-walled carbon nanotubes (SWNTs) are of great interest due to their unique physical and chemical properties. Most applications of SWNTs need to have a very high purity of SWNTs; hence, the purification of SWNTs was focused on in this study. In this research, the first step of removing silica by concentrated NaOH and the second step of recovering NaOH-treated SWNTs by froth flotation were studied. To achieve a high removal efficiency of froth flotation, a surfactant concentration of 0.75 times the CMC was selected to avoid silica entrainment to the top of the column; whereas a sonication time of 3 h during the silica dissolution step, a sample loading of 1.0 mg/ml, an air flow rate of 100 ml/min, and a foam height of 22 cm yielded a maximum carbon content of about 78%, while the selectivity to SWNTs on the samples in the range of 71% indicates that most of the SWNTs in the sample were recovered by a combination of NaOH leaching and froth flotation. This study has demonstrated that combining silica dissolution and froth flotation can be used to purify and concentrate the SWNTs synthesized by the disproportionation of CO over a Co-Mo/SiO₂ catalyst without damage to the physical structures of the SWNTs.

7.6 Acknowledgements

The Thailand Research Fund (TRF) is acknowledged for providing a research grant and the Royal Golden Jubilee Ph.D. fellowships PHD/0127/2544. The National Excellence Center for Petroleum, Petrochemical and Advanced Materials, under The Ministry of Education, Thailand and The Research Unit: Applied Surfactants for Separation and Pollution Control, under The Ratchadapiseksompote Fund, Chulalongkorn University, are also acknowledged for providing research facilities and funding, respectively.

7.7 REFERENCES

- [1] S. Iijima, T. Ichihashi, Single-shell carbon nanotubes of 1-nm diameter, *Nature* 363 (1993) 603-605.
- [2] E. Gregan, S.M. Keogh, A. Maguire, T.G. Hedderman, L.O. Neill, G. Chambers, H.J. Byrne, Purification and isolation of SWNTs, *Carbon* 42 (2004) 1031-1035.
- [3] W. Tang, M.H. Santare, S.G. Advani, Melt processing and mechanical property characterization of multi-walled carbon nanotube/high density polyethylene (MWNT/HDPE) composite films, *Carbon* 41 (2003) 2779-2785.
- [4] D.S. Bethune, C.H. Kiang, M.S. de Vries, G. Gorman, R. Savoy, J. Vazquez, R. Beyers, Cobalt-catalysed growth of carbon nanotubes with single-atomic-layer walls, *Nature* 363 (1993) 605-607.
- [5] T. Guo, P. Nikolaev, A. Thess, D.T. Colbert, R.E. Smalley, Catalytic growth of single-walled nanotubes by laser vaporization, *Chem. Phys. Lett.* 243 (1995) 49-54.
- [6] B. Kitiyanan, W.E. Alvarez, J.H. Harwell, D.E. Resasco, Controlled production of single-wall carbon nanotubes by catalytic decomposition of CO on bimetallic Co-Mo catalysts, *Chem. Phys. Lett.* 317 (2000) 497-503.
- [7] J.E. Herrera, L. Balzano, A. Borgna, W.E. Alvarez, D.E. Resasco, Relationship between the structure/composition of Co-Mo catalysts and their ability to produce single-walled carbon nanotubes by CO disproportionation, *J. Catal.* 204 (2001) 129-145.
- [8] O. Matarredona, H. Rhoads, Z. Li, J.H. Harwell, L. Balzano, D.E. Resasco, Dispersion of single-walled carbon nanotubes in aqueous solutions of the anionic surfactant NaDDBS, *J. Phys. Chem. B* 107 (2003) 13357-13367. HF+NaOH

- [9] I.W. Chiang, B.E. Brinson, A.Y. Huang, P.A. Willis, M.J. Bronikowski, J.L. Margrave, R.E. Smalley, R.H. Hauge, Purification and characterization of single-wall carbon nanotubes (SWNTs) obtained from the gas-phase decomposition of CO (HiPco Process), *J. Phys. Chem. B* 105 (2001) 8297-8301. HCl
- [10] A.C. Dillon, T. Gennet, K.M. Jones, J.L. Alleman, P.A. Parilla, M.J. Heben, A simple and complete purification of single-walled carbon nanotube materials, *Adv. Mater.* 11 (1999) 1354-1358.
- [11] I.W. Chiang, B.E. Brison, R.E. Smalley, J.L. Margrave, R.H. Hauge, Purification and characterization of single-wall carbon nanotubes, *J. Phys. Chem. B* 105 (2001) 1157-1161. HNO₃+HCl
- [12] H. Igarashi, H. Murakami, Y. Murakami, S. Maruyama, N. Nakashima, Purification and characterization of zeolite-supported single-walled carbon nanotubes catalytically synthesized from ethanol, *Chem. Phys. Lett.* 392 (2004) 529-532. HF
- [13] <http://www.epicindustries.com/msds/Epi%20Sour%20All%20MSDS.doc>, accessed August 2006
- [14] D.W. Fuerstenau, R. Herrera-Urbina, Mineral separation by froth flotation, in: J.F. Scamehorn, J.H. Harwell (Eds.), *Surfactant-based separation processes*, Marcel Dekker, New York, 1989, pp. 259-320.
- [15] B. Yarar, Flotation, in: D.M. Ruthven (Ed), *Encyclopedia of separation technology Vol. 2*, John Wiley & Sons, New York, 1997, pp. 913-939.
- [16] A.I. Zouboulis, N.K. Lazaridis, D. Zamboulis, Powdered activated carbon separation from water by foam flotation, *Sep. Sci. Technol.* 29 (1994) 385-400.
- [17] S. Chavadej, P. Ratanarojanatam, W. Phoochinda, U. Yanatatsaneejit, J.F. Scamehorn, Clean-up of oily wastewater by froth flotation: Effect of microemulsion

formation II: Use of anionic/nonionic surfactant mixtures, *Sep. Sci. Technol.* 39 (2004) 3079-3096.

[18] P. Chungchamroenkit, S. Chavadej, U. Yanatatsaneejit, B. Kitiyanan, J.F. Scamehorn, Separation of carbon black from silica by froth flotation, Submitted to *Sep. Sci. Technol.*

[19] D.E. Resasco, W.E. Alvarez, F. Pompeo, L. Balzano, J.E. Herrera, B. Kitiyanan, A. Borgna, A scalable process for production of single-walled carbon nanotubes (SWNTs) by catalytic disproportionation of CO on a solid catalyst, *J. Nanopart. Res.* 4 (2002) 131-136.

[20] W.E. Alvarez, B. Kitiyanan, A. Borgna, D.E. Resasco, Synergism of Co and Mo in the catalytic production of single-wall carbon nanotubes by decomposition of CO, *Carbon* 39 (2001) 547-558.

[21] M.J. Rosen, *Surfactant and interfacial phenomena*, 2nd ed., John Wiley & Sons, New York, 1989, pp. 276-303.

[22] Y. Zhao, Y. Deng, J.Y. Zhu, Roles of surfactants in flotation deinking, *Prog. Pap. Recycl.* 14 (2004) 41-45.

[23] U. Yanatatsaneejit, A. Withayapanyanon, P. Ransunvigit, E.J. Acosta, D.A. Sabatini, J.F. Scamehorn, S. Chavadej, Ethylbenzene removal by froth flotation under conditions of middle-phase microemulsion formation I: Interfacial tension, foamability, and foam stability, *Sep. Sci. Technol.* 40 (2005) 1537-1553.

[24] U. Yanatatsaneejit, P. Ransunvigit, J.F. Scamehorn, S. Chavadej, Diesel removal by froth flotation under low interfacial tension conditions I: Foam characteristics, coalescence time, and equilibration time, Submitted to *Sep. Sci. Technol.*

- [25] J.F. Scamehorn, D.A. Sabatini, J.H. Harwell, Surfactants, Part II: Applications, in: J. Atwood, J. Stead (Eds.), Encyclopedia of supramolecular chemistry, Marcel Dekker, Inc., New York, 2004, pp. 1470-1477.
- [26] A.W. Adamson, Physical chemistry of surfaces, 4th ed., Wiley, New York, 1982, pp. 349.
- [27] H.A.E. Mulleneers, L.K. Koopal, G.C.C. Swinkels, H. Bruning, W.H. Rulkens, Flotation of soot particles from a sandy soil sludge, Colloids Surf., A. 151 (1999) 293-301.
- [28] P.A. Kralchevsky, K. Nagayama, Particles at fluid interfaces and membranes, Elsevier, Amsterdam, 2001, pp. 591-633.
- [29] M.M. Koutlemani, P. Mavros, A.I. Zouboulis, K.A. Matis, Recovery of Co^{2+} ions from aqueous solutions by froth flotation, Sep. Sci. Technol. 29 (1994) 867-886.
- [30] U. Yanatatsaneejit, S. Chavadej, P. Rangsunvigit, J.F. Scamehorn, Ethylbenzene removal by froth flotation under conditions of middle-phase microemulsion formation II: Effects of air flow rate, oil-to-water ratio, and equilibration time, Sep. Sci. Technol. 40 (2005) 1629-1620.
- [31] A.M. Rao, E. Richter, S. Bandow, B. Chase, P.C. Eklund, K.A. Williams, S. Fang, K.R. Subbaswamy, M. Menon, A. Thess, R.E. Smalley, G. Dresselhaus, M.S. Dresselhaus, Diameter-selective Raman scattering from vibrational modes in carbon nanotubes, Science 275 (1997) 187-191.
- [32] S. Noda, H. Sugime, T. Osawa, Y. Tsuji, S. Chiashi, Y. Murakami, S. Maruyama, A simple combinatorial method to discover Co-Mo binary catalysts that grow vertically aligned single-walled carbon nanotubes, Carbon 44 (2006) 1414-1419.